Multi-loop periodic event-triggered actuation: applications to PID, cascade, and decoupling control

Takuya Iwaki, Emilia Fridman & Karl Henrik Johansson

Published online: 03 Jan 2022.

Submit your article to this journal

Article views: 910

View related articles

View Crossmark data

OPEN ACCESS Check for updates

Multi-loop periodic event-triggered actuation: applications to PID, cascade, and decoupling control

Takuya Iwaki [a], Emilia Fridman [b] and Karl Henrik Johansson [a]

[a]School of Electrical Engineering and Computer Science, KTH Royal Institute of Technology, Stockholm, Sweden; [b]School of Electrical Engineering, Tel-Aviv University, Tel Aviv, Israel

ABSTRACT

This paper studies periodic event-triggered actuation applied to PID, cascade, and decoupling control. We propose an event-triggered output feedback controller, in which the control command is actuated only when it exceeds its previous value by a certain threshold. An exponential stability condition is derived in the form of LMIs using a Lyapunov–Krasovskii functional based on Wirtinger's inequality. It is shown that an observer-based controller can reject an unknown step disturbance. Using this result, we propose a way to tune the event threshold subject to a given stability margin. We apply the proposed framework to PID, cascade, and decoupling control to illustrate how the event thresholds can be tuned in practice. Numerical examples show for these three control architectures how controller–actuator communication can be reduced without performance degradation.

1. Introduction

Process control over wireless communication is of growing interest with the recent development of wireless technology (Ahlén et al., 2019; Isaksson et al., 2017; Park et al., 2018; Samad et al., 2007). A key to realizing wireless process control is to guarantee control performance under limited sensor and actuator communications. In this context, event-triggered control has attracted much attention (Heemels et al., 2012). The main purpose of this paper is to develop and apply event-triggered actuation to PID, cascade, and decoupling control, which are frequent architectures for process control systems.

1.1 Motivation

Process plants are complex systems producing a wide variety of industrial products, such as oil, gas, chemical, steel, paper, and food. Since these products are essential to our society, process plants need to operate properly to satisfy economic, environmental, and safety requirements. Process control systems enable such operations by regulating process variables such as temperature, pressure, level, and flow rate often through multiple PID control loops. For example, consider the Swedish paper plant in Iggesund (Ahlén et al., 2019). It includes a subunit called a starch cooker to produce starch pastes used to coat the papers. The starch cooker is controlled by seven PID control loops to obtain the starch pastes with the desired concentration. Another example is a distillation column, the main subunit of oil and gas refinery plants (Seborg et al., 2010). It separates a mixture into light and heavy components. To properly separate the mixture, the temperatures at the top and bottom of the column are regulated by adjusting the reflux and boiler steam flow rate. A distillation control system mainly consists of two PID control loops. In these two examples, PID controllers often independently regulate the corresponding process variables to make the subunits function properly.

In process control systems, feedforward control is used together with PID control to compensate for external disturbances when they can be measured explicitly. Using the information from the disturbance sensor, the controller takes corrective action before the controlled variable deviates too much from its setpoint. Multi-loop control architectures, such as cascade and decoupling control, are also often introduced to enhance the control performance (Åström & Hägglund, 2006; Seborg et al., 2010). If disturbances cannot be measured and are associated with a control signal, cascade control can be considered. Cascade control employs another controller so that it provides a tighter inner control loop. Decoupling control is introduced between two independent PID control loops when their control signal variations interact with each other. They adjust the corresponding control signals so that the interactions are mitigated proactively.

Two wireless communication standards that have been proposed for process control systems are WirelessHART (HART Communication Foundation, 2014) and ISA-100 (International Society of Automation, 2009). Both employ a mesh-structured multi-hop network, in which the network nodes consist of wireless sensors, actuators, and gateways (Figure 1). Wireless process control offers advantages through potentially massive sensing, flexible deployment and operation, and efficient maintenance. However, there remains the problem how to limit the amount of information that needs to be exchanged over the network since system performance is critically affected by network-induced
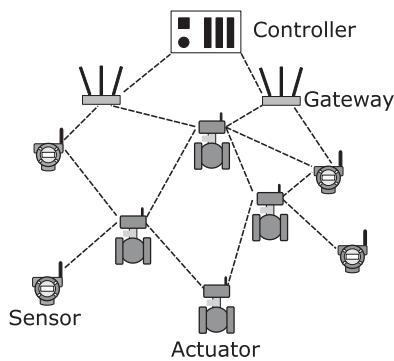
CONTACT Takuya Iwaki ✉ takya@kth.se School of Electrical Engineering and Computer Science, KTH Royal Institute of Technology, Malvinas väg 10, Floor 6, Stockholm 100 44, Sweden

Figure 1. Architecture of wireless process control systems.

delay, packet dropout, communication outages, and battery shortage of wireless devices. Resource-aware communication and control strategies, therefore, need to be investigated.

1.2 Related work

Aperiodic control systems have been investigated as a measure to reduce the communication load of wireless networks. In Araújo et al. (2014), aperiodic sampling strategies under the wireless medium access control (MAC) protocol are proposed. The framework is experimentally evaluated on a double-tank system, which mimics typical industrial process control loops. In Di Girolamo and D'Innocenzo (2019), the authors focus on how to design a controller and scheduler for WirelessHART. A co-design framework of a controller and scheduler is proposed by formulating an optimal control problem under multi-hop network communication.

In event-triggered control, sensor measurements or control signals are transmitted to the corresponding network nodes only when a given condition is satisfied so that the usage of communication can be significantly reduced (Årzén, 1999; Åström & Bernhardsson, 1999). Many event-triggered control strategies have been proposed and investigated (Heemels et al., 2012). To suit for practical implementation, periodic event-triggered control is proposed in Heemels et al. (2012) and Heemels and Donkers (2013). Since the event trigger only needs to check the event-triggering condition periodically, a minimum event time is guaranteed.

Many researchers have studied event-triggered control for industrial processes. Most studies focus on analyzing and designing event-triggered PI or PID control since PID control is still the first choice for process control. Stability conditions for PI control subject to actuator saturation are derived in Kiener et al. (2014) and Moreira et al. (2019). Event-triggered PI control for first-order systems using the PIDPLUS implementation (Song et al., 2006) is discussed in Tiberi et al. (2012). In Selivanov and Fridman (2018), a time-delay approach is used to derive a stability condition of periodic event-triggered PID control, where the control signal is updated when its relative value goes beyond a given threshold. Experimental validation is carried out in Kiener et al. (2014) and Lehmann and Lunze (2011). Implementations on a real industrial plant are presented in Blevins et al. (2015), Lindberg and Isaksson (2015) and Norgren et al. (2012).

The objective of PID control is in most cases setpoint tracking or disturbance rejection (Åström & Hägglund, 2006). These properties of event-triggered PID control have been investigated. For setpoint tracking, it is shown that the output converges to a constant when the setpoint value and the controller state are available at the sensor (Reimann et al., 2015; Tiberi et al., 2012). In Lehmann and Johansson (2012), the authors show that event-triggered PI control has bounded responses for setpoint tracking and disturbance rejection. Observer-based event-triggered control for disturbance rejection is proposed in Garcia and Antsaklis (2014) and Wang et al. (2017). In these studies, it is required to have the capability to imitate the controller or to implement an observer at the wireless sensors, which is intrinsically difficult to realize if the controller uses measurements from multiple sensors generated at different locations. For example, this is the case in cascade control and decoupling control, where the measurements from two sensors need to be used to implement the controller and observer. In wireless process control systems, the sensors are typically distributed over an area, and the measurements are transmitted to the controller through a multi-hop wireless network (Figure 1). The controller is the only place where all the information is available. In Tiberi et al. (2012), a self-triggered control strategy is introduced where the event trigger is located at the controller. While both setpoint tracking and disturbance rejection are investigated, the application is limited to first-order systems.

1.3 Contribution

This paper proposes an event-triggered actuation framework for PID control, cascade, and decoupling control. We consider event-triggered output feedback control for a continuous-time linear system, where the plant state is measured periodically by multiple sampled-data sensors. The control signal is sent to the actuator in a periodic event-triggered fashion. Since the control signal is transmitted through a multi-hop network, the sensors and actuators consume energy as relay nodes. Our strategy effectively reduces the communication load in the network but also the number of control command changes. The controller updates the signal to the actuator when its value goes beyond a given threshold.

The main contributions of this paper are outlined as follows:

- We introduce a general event-triggered output feedback control system with delayed sampling. An exponential stability condition is derived using a Lyapunov–Krasovskii functional based on Wirtinger's inequality (Theorem 3.1).
- By modifying the event-triggering condition and introducing an observer, we show that the proposed controller achieves setpoint tracking and disturbance rejection (Theorems 3.2 and 3.3).
- A tuning procedure is provided for the event threshold under a given stability margin (Corollary 3.1). The optimal threshold is obtained by solving a semi-definite programming (SDP) problem.
- We apply this framework to PID control as well as cascade and decoupling control. Numerical examples for each case are presented to illustrate how to tune the event thresholds.

The examples show that our proposed framework reduces the communication loads without performance degradation.

1.4 Outline

The remainder of this paper is organized as follows. Section 2 introduces the plant model and formulates the problem considered. In Section 3, we derive the stability condition of the proposed event-triggered control. Setpoint tracking and disturbance rejection properties are also investigated. Applications to PID, cascade, and decoupling control are discussed in Section 4. Numerical examples for each controller are also provided. The conclusion is presented in Section 5.

1.5 Notation

Throughout this paper, $\mathbb{N}$, $\mathbb{N}_0$, and $\mathbb{R}$ are the sets of integers larger than zero, nonnegative integers, and real numbers, respectively. The set of n by n positive definite (positive semi-definite) matrices over $\mathbb{R}^{n \times n}$ is denoted as $\mathbb{S}_{++}^n$ ($\mathbb{S}_+^n$). For simplicity, we write $X > Y$ ($X \geq Y$), $X, Y \in \mathbb{S}_{++}^n$, if $X - Y \in \mathbb{S}_{++}^n$ ($X - Y \in \mathbb{S}_+^n$) and $X > 0$ ($X \geq 0$) if $X \in \mathbb{S}_{++}^n$ ($X \in \mathbb{S}_+^n$). Symmetric matrices of the form $\begin{bmatrix} A & B \\ B^\top & C \end{bmatrix}$ are written as $\begin{bmatrix} A & B \\ * & C \end{bmatrix}$ with $B^\top$ denoting the transpose of B.

2. System model and problem formulation

In this section, we formulate the problem considered. We first introduce a plant model given by a continuous-time linear system. A PID controller is then introduced together with cascade and decoupling controllers. Finally, the event trigger problem studied in this paper is formulated.

2.1 System model

Consider a continuous-time linear plant measured by N sensors given by

$$\dot{x}_p(t) = A_p x_p(t) + B_p \tilde{u}(t_k) + B_d d(t), \quad t \in [t_k, t_{k+1}), \quad (1)$$

$$y_i(t) = C_p^i x_p(t), \quad i \in \mathcal{N} \triangleq \{1, \dots, N\}, \quad (2)$$

where $x_p(t) \in \mathbb{R}^{n_p}$, $\tilde{u}(t) \in \mathbb{R}^m$, $d(t) \in \mathbb{R}^{n_d}$ and $y_i(t) \in \mathbb{R}$ are the state, event-triggered control signal applied to the actuator, disturbance, and output of sensor i, respectively. We assume that the controller updates its state and control signal (defined below for each controller) every h_0 time interval, and let t_k be the time of update $k \in \mathbb{N}_0$ of the controller, i.e. $t_k = kh_0$ for all $k \in \mathbb{N}_0$. Sensor i samples and transmits its measurement every h_i time interval. The control signal is computed based on the measurements from sensor $y_i(s_i(t_k)), i \in \mathcal{N}$ and $r(t_k)$ where $s_i(t_k)$ is the last transmission time of sensor i at time t_k. That is, we have $s_i(t_k) = \ell_i h_i$ where $\ell_i = \lfloor t_k/h_i \rfloor$.

We especially consider three controllers: PID, cascade, and decoupling controllers. Their state-space formulations are given as follows.

PID control

The block diagram of event-triggered PID control is shown in Figure 2(a). Note that PID control includes a single sensor, i.e.

$N = 1$. A standard PID controller can be written as

$$\dot{x}_c(t) = r(t_k) - y_1(s_1(t_k)), \quad t \in [t_k, t_{k+1}), \quad (3)$$

$$u(t) = K_\mathrm{p}(br(t_k) - y_1(s_1(t_k))) + K_\mathrm{i} x_c(t_k)$$
$$+ K_\mathrm{d}(c\Delta r(t_k) - \Delta y_1(s_1(t_k))), \quad (4)$$

where $K_\mathrm{p}, K_\mathrm{i}, K_\mathrm{d}$ are proportional, integral, and derivative gains, respectively, and b, c, weight parameters. For the derivative term, we use the backward Euler method, i.e.

$$\Delta y_i(s_i(t_k)) = \frac{1}{h_i}\left(y_i(s_i(t_k)) - y_i(s_i(t_k) - h_i)\right), \quad i \in \mathcal{N},$$

$$\Delta r(t_k) = \frac{1}{h_0}\left(r(t_k) - r(t_k - h_0)\right).$$

The derivative term is usually implemented with a first-order filter (Åström & Hägglund, 2006). In this case, the controller state, consisting of the integrator and derivative filter, is given by

$$\dot{x}_{c,1}(t) = r(t_k) - y_1(s_1(t_k)), \quad (5)$$

$$\dot{x}_{c,2}(t) = -\frac{1}{T_1}x_{c,2}(t_k) + \frac{1}{T_1}(c\Delta r(t_k) - \Delta y_1(s_1(t_k))), \quad (6)$$

$$u(t) = K_\mathrm{p}(br(t_k) - y_1(s_1(t_k))) + K_\mathrm{i} x_{c,1}(t_k) + K_\mathrm{d} x_{c,2}(t_k), \quad (7)$$

where $x_{c,1}(t), x_{c,2}(t)$ is the integrator and the filter states, respectively, of the PID controller, and T_1 is the filter's time constant.

Cascade control

In cascade control (Figure 2(b)), the outer PID controller computes its control signal for reference of the inner controller. The inner controller sends its signal to the actuator, i.e.

$$\dot{x}_{c,1}(t) = r(t_k) - y_1(s_1(t_k)),$$

$$\dot{x}_{c,2}(t) = -\frac{1}{T_1}x_{c,2}(t_k) + \frac{1}{T_1}(c\Delta r(t_k) - \Delta y_1(s_1(t_k))),$$

$$\dot{x}_{c,3}(t) = v(t_k) - y_2(s_2(t_k)),$$

$$\dot{x}_{c,4}(t) = -\frac{1}{T_2}x_{c,4}(t_k) - \frac{1}{T_2}\Delta y_2(s_2(t_k)),$$

$$v(t) = bK_\mathrm{p}^1(r(t_k) - y_1(s_1(t_k))) + K_\mathrm{i}^1 x_{c,1}(t_k) + K_\mathrm{d}^1 x_{c,2}(t_k),$$

$$u(t) = K_\mathrm{p}^2(v(t_k) - y_2(s_2(t_k))) + K_\mathrm{i}^2 x_{c,3}(t_k) + K_\mathrm{d}^2 x_{c,4}(t_k),$$

where $x_{c,1}(t), x_{c,2}(t)$ are the integrator and filter states, respectively, of the outer PID controller, $x_{c,3}(t), x_{c,4}(t)$ those of the inner PID controller, $K_\mathrm{p}^i, K_\mathrm{i}^i, K_\mathrm{d}^i, T_i, i = 1, 2$, are the corresponding proportional, integral, and derivative gains, and the filter's time constants.

Remark 2.1: The inner controller is given by setting $b = 1$ and $c = 0$ in PID control (5)–(7). This form is suitable for rejecting input disturbance.

Decoupling control

In decoupling control (Figure 2(c)), two PID controllers are interconnected. The controller dynamics is given by

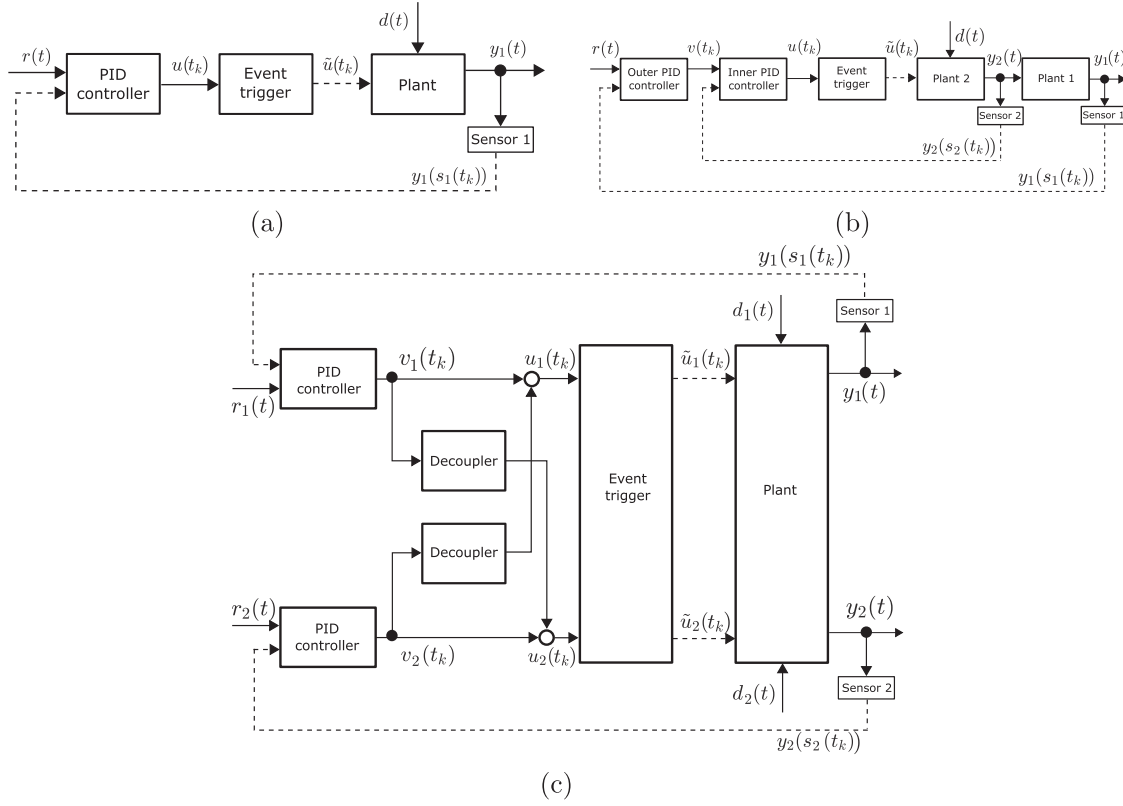$$\dot{x}_{c,1}(t) = r_1(t_k) - y_1(s_1(t_k)),$$

Figure 2. Block diagrams of event-triggered PID, cascade, and decoupling control. (a) PID control (b) Cascade control (c) Decoupling control .

$$\dot{x}_{c,2}(t) = -\frac{1}{T_1}x_{c,2}(t_k) + \frac{1}{T_1}(c_1\Delta r(t_k) - \Delta y_1(s_1(t_k))),$$

$$\dot{x}_{c,3}(t) = r_2(t_k) - y_2(s_2(t_k)),$$

$$\dot{x}_{c,4}(t) = -\frac{1}{T_2}x_{c,4}(t_k) + \frac{1}{T_2}(c_2\Delta r(t_k) - \Delta y_2(s_2(t_k))),$$

$$v_1(t) = K_p^1(r_1(t_k) - y_1(s_1(t_k))) + K_i^1 x_{c,1}(t_k) + K_d^1 x_{c,2}(t_k),$$

$$v_2(t) = K_p^2(r_2(t_k) - y_2(s_2(t_k))) + K_i^2 x_{c,3}(t_k) + K_d^2 x_{c,4}(t_k),$$

$$u_1(t) = v_1(t_k) + K_g^1 v_2(t_k),$$

$$u_2(t) = v_2(t_k) + K_g^2 v_1(t_k),$$

where $x_{c,1}(t), x_{c,2}(t)$ are the integrator and filter states, respectively, of PID controller 1, $x_{c,3}(t), x_{c,4}(t)$ those of controller 2. The parameters $K_p^i, K_i^i, K_d^i, K_g^i, T_i, b_i, c_i, i = 1, 2$, are the corresponding proportional, integral, derivative, decoupler gains, time constants, and weights, respectively.

2.2 Problem formulation

Next, we formulate the problem considered in this paper. Considering a plant given by (1)–(2), together with PID, cascade, or decoupling control, this paper aims to obtain an event-triggered actuation framework based on periodic event-triggered control. The event-triggering condition is given by

$$(u(t_k) - \tilde{u}(t_{k-1}))^\top \Omega (u(t_k) - \tilde{u}(t_{k-1})) > \sigma u^\top(t_k)\Omega u(t_k) + \rho \tag{8}$$

where $\sigma \geq 0$ is a relative threshold, $\Omega \in \mathbb{S}_{++}^m$ a matrix, and $\rho > 0$ a constant, all to be determined. The event-triggered control signal is given by

$$\tilde{u}(t) = \begin{cases} u(t_k), \ t \in [t_k, t_{k+1}), & \text{if (8) is true,} \\ \tilde{u}(t_{k-1}), \ t \in [t_k, t_{k+1}), & \text{if (8) is false,} \end{cases} \tag{9}$$

with $\tilde{u}_0 = u(t_0)$.

Remark 2.2: The positive constant ρ excludes Zeno behavior for continuous event-triggered control (Donkers & Heemels, 2012). For periodic event-triggered control, we can derive an exponential stability condition when $\rho = 0$. A small ρ can reduce the event generation.

To handle all controllers introduced above in a general form, we introduce an output feedback controller given by

$$\dot{x}_c(t) = A_c x_c(t_k) + \sum_{i \in \mathcal{N}} B_c^i y_i(s_i(t_k)) + \sum_{i \in \mathcal{N}} \bar{B}_c^i y_i(s_i(t_k) - h_i)$$
$$+ B_r r(t_k) + \bar{B}_r r(t_k - h_0), \quad t \in [t_k, t_{k+1}), \tag{10}$$

$$u(t) = C_c x_c(t_k) + \sum_{i \in \mathcal{N}} D_c^i y_i(s_i(t_k)) + \sum_{i \in \mathcal{N}} \bar{D}_c^i y_i(s_i(t_k) - h_i)$$
$$+ D_r r(t_k) + \bar{D}_r r(t_k - h_0), \tag{11}$$

where $x_c(t) \in \mathbb{R}^{n_c}$ is the controller state. By augmenting the state $x(t) = [x_p^\top(t), x_c^\top(t)]^\top \in \mathbb{R}^n$ with $n \triangleq n_p + n_c$, we have

the following closed-loop system description

$$\dot{x}(t) = Ax(t) + A_0 x(t_k) + \sum_{i \in \mathcal{N}} A_i x(s_i(t_k))$$

$$+ \sum_{i \in \mathcal{N}} \bar{A}_i x(s_i(t_k) - h_i)$$

$$+ B\xi(t) + B_D d(t) + B_R r(t_k) + \bar{B}_R r(t_k - h_0) \quad (12)$$

where

$$\xi(t) \triangleq \tilde{u}(t) - u(t)$$
$$= \tilde{u}(t_k) - u(t_k), \quad t \in [t_k, t_{k+1}),$$

is the control signal error due to event-triggered actuation, and the matrices are given by

$$A = \begin{bmatrix} A_p & 0 \\ 0 & 0 \end{bmatrix}, \quad A_0 = \begin{bmatrix} 0 & B_p C_c \\ 0 & A_c \end{bmatrix}, \quad A_i = \begin{bmatrix} B_p D_c^i C_p^i & 0 \\ B_c^i C_p^i & 0 \end{bmatrix},$$

$$\bar{A}_i = \begin{bmatrix} B_p \bar{D}_c^i C_p^i & 0 \\ \bar{B}_c^i C_p^i & 0 \end{bmatrix}, \quad B = \begin{bmatrix} B_p \\ 0 \end{bmatrix}, \quad B_D = \begin{bmatrix} B_d \\ 0 \end{bmatrix},$$

$$B_R = \begin{bmatrix} B_p D_r \\ B_r \end{bmatrix}, \quad \bar{B}_R = \begin{bmatrix} B_p \bar{D}_r \\ \bar{B}_r \end{bmatrix}.$$

We formulate the problem as follows: Consider the system (12) under PID, cascade, or decoupling control. How to design the event trigger (8)–(9) such that the closed-loop system (12) is exponentially stable with a given convergence rate and has setpoint tracking and disturbance rejection capabilities?

Remark 2.3: This paper studies the event-triggered actuation. While the sensor measurements are still periodically sampled and transmitted, we can expect to reduce the communication load since we mainly focus on the multi-hop wireless network (Figure 1) introduced in the process control application. In multi-hop networks, the control signals are also transmitted through some intermittent wireless network nodes such as wireless sensors and actuators. Thus, reducing controller–actuator communication results in saving the energy consumption of the intermittent nodes between the controller and the corresponding actuator.

3. Main results

In this section, we present the main results of this paper. First, we derive a stability condition of time-triggered output feedback control in Lemma 3.1. We then discuss event-triggered control. Next, setpoint tracking and disturbance rejection properties are considered. We also discuss how to tune the event trigger parameters.

3.1 Stability analysis

We first derive the stability condition of the time-triggered control system given by system (12) with $\xi(t) \equiv 0$. Define the

following matrices:

$$\bar{A} \triangleq A + A_0 + \sum_{i \in \mathcal{N}} A_i, \quad \tilde{A} \triangleq \bar{A} + \sum_{i \in \mathcal{N}} \bar{A}_i,$$

$$K_0 \triangleq \begin{bmatrix} 0 & C_c \end{bmatrix}, \quad K_i = \begin{bmatrix} D_c^i C_p^i & 0 \end{bmatrix}, \quad \bar{K}_i \triangleq \begin{bmatrix} \bar{D}_c^i C_p^i & 0 \end{bmatrix},$$

$$\bar{K} \triangleq K_0 + \sum_{i \in \mathcal{N}} K_i, \quad \tilde{K} \triangleq \bar{K} + \sum_{i \in \mathcal{N}} \bar{K}_i, \quad K_R = D_r, \quad \bar{K}_R = \bar{D}_r.$$

Lemma 3.1: *Consider the closed-loop system* (12) *with* $\xi(t) \equiv d(t) \equiv r(t) \equiv 0$. *Assume that there exist* $P, W_0, W_i, \bar{W}_i, Q_i, R_i \in \mathbb{S}_{++}^n, i \in \mathcal{N}$, *and* $\alpha > 0$, *such that* $\Phi = \Phi^\top = \{\Phi_{j\ell}\} < 0$ *where*

$$\Phi_{11} = P\bar{A} + \bar{A}^\top P + 2\alpha P + \sum_{i \in \mathcal{N}} \left[Q_i - e^{-2\alpha h_i} R_i \right],$$

$$\Phi_{1(i+1)} = P\bar{A}_i + e^{-2\alpha h_i} R_i, \quad i = 1, \ldots, N,$$

$$\Phi_{1(i+N+2)} = PA_i, \quad i = 1, \ldots, N,$$

$$\Phi_{1(i+2N+2)} = P\bar{A}_i, \quad i = 1, \ldots, N,$$

$$\Phi_{1(3N+2)} = \bar{A}^\top S,$$

$$\Phi_{(i+1)(i+1)} = -e^{-2\alpha h_i}(Q_i + R_i), \quad i = 1, \ldots, N,$$

$$\Phi_{(i+1)(3N+3)} = \bar{A}_i^\top S, \quad i = 1, \ldots, N,$$

$$\Phi_{(i+N+2)(i+N+2)} = -\frac{\pi^2}{4} W_i, \quad i = 0, 1, \ldots, N,$$

$$\Phi_{(i+N+2)(3N+3)} = A_i^\top S, \quad i = 0, 1, \ldots, N,$$

$$\Phi_{(i+2N+2)(i+2N+2)} = -\frac{\pi^2}{4} e^{-2\alpha h_i} \bar{W}_i, \quad i = 1, \ldots, N,$$

$$\Phi_{(i+2N+2)(3N+3)} = -\bar{A}_i^\top S, \quad i = 1, \ldots, N,$$

$$\Phi_{(3N+3)(3N+3)} = -S,$$

with

$$S \triangleq h_0^2 e^{-2\alpha h_0} W_0 + \sum_{i \in \mathcal{N}} \left[(h_0 + h_i)^2 e^{-2\alpha(h_0 + h_i)} \right.$$
$$\left. \times (W_i + \bar{W}_i) + h_i^2 R_i \right],$$

and the other elements are zero matrices. Then the closed-loop system (12) *is exponentially stable with decay rate* α.

Proof: See Appendix 1. ∎

We then have the following stability condition for the event-triggered control systems.

Theorem 3.1: *Consider the closed-loop system* (12) *with* $d(t) \equiv r(t) \equiv 0$ *and the event trigger* (8)–(9) *with* $\rho = 0$. *Assume that there exist* $P, W_0, W_i, \bar{W}_i, Q_i, R_i \in \mathbb{S}_{++}^n, i \in \mathcal{N}, w > 0, \sigma > 0,$

and $\alpha > 0$, such that

$$
\Psi \triangleq \left[\begin{array}{ccccc|cc}
 & & & & & PB & w\sigma \bar{K}^{\top}\Omega \\
 & & & & & 0 & w\sigma \bar{K}_1^{\top}\Omega \\
 & & & & & \vdots & \vdots \\
 & & & & & 0 & w\sigma \bar{K}_N^{\top} \\
 & & & & & 0 & w\sigma K_0^{\top}\Omega \\
 & & \Phi & & & \vdots & \vdots \\
 & & & & & 0 & w\sigma K_N^{\top}\Omega \\
 & & & & & 0 & w\sigma \bar{K}_1^{\top}\Omega \\
 & & & & & \vdots & \vdots \\
 & & & & & 0 & w\sigma \bar{K}_N^{\top}\Omega \\
 & & & & & SB & 0 \\
\hline
* & * & \cdots & * & * & -w\Omega & 0 \\
* & * & \cdots & * & * & 0 & -w\sigma\Omega
\end{array}\right] < 0. \quad (13)
$$

Then the closed-loop system (12) *is exponentially stable with decay rate α.*

Proof: See Appendix 2. ∎

Remark 3.1: This paper considers the event trigger with respect to the control signal. The event trigger for the plant output can be considered by replacing $y(s_i(t_k))$, $y(s_i(t_k - h_i))$ by $\tilde{y}(s_i(t_k)) = y(s_i(t_k)) + e_i(s_i(t_k))$, $\tilde{y}(s_i(t_k) - h_i) = y(s_i(t_k) - h_i) + e_i(s_i(t_k) - h_i)$ in (10)–(11). This may further reduce communication load but requires to introduce more terms when considering the derivative of the Lyapunov functional. This results in more complicated LMI with additional block-columns and block-rows. In this paper, we consider only the event-triggered actuation for simplicity.

3.2 Setpoint tracking and disturbance rejection

In the previous subsection, we provided a stability condition of event-triggered control without reference signals or disturbances. In this case, the equilibrium point of the closed-loop system (12) is the origin. However, when there is a constant reference signal or disturbance, each element of the augmented state $x(t)$ converges possibly to a non-zero value even if the event-triggered controller successfully stabilizes the plant. The steady-state control signal may also be non-zero, which causes a tracking error even if the controller contains an integrator. This fact imposes modification of the event-triggering condition. Considering this, we discuss setpoint tracking and disturbance rejection of event-triggered control. We assume that the reference signal and disturbance changes are sufficiently slow compared to the plant dynamics and hence can be regarded as constants.

First, setpoint tracking is considered. We show the following lemma.

Lemma 3.2: *If $\Psi < 0$, then $\tilde{A}$ is invertible.*

Proof: Let us denote

$$
\zeta = [\underbrace{x^{\top}, \ldots, x^{\top}}_{N+1}, 0, \ldots, 0]^{\top}
$$

where $x \in \mathbb{R}^n$ is an arbitrary non-zero vector. Then we have

$$
\zeta^{\top}\Psi\zeta
$$
$$
= x^{\top}\left(P\tilde{A} + \tilde{A}^{\top}P + 2\alpha P + \sum_{i\in\mathcal{N}}\left[1 - e^{-2\alpha h_i}Q_i\right]\right)x < 0.
$$

Since $1 - e^{-2\alpha h_i} > 0$ for $h_i > 0$, $\tilde{A}$ is Hurwitz, and therefore, invertible. ∎

Consider the updated event-triggering condition

$$
(u(t_k) - \tilde{u}(t_{k-1}))^{\top}\Omega(u(t_k) - \tilde{u}(t_{k-1}))
$$
$$
> \sigma(u(t_k) - u_c(t_k))^{\top}\Omega(u(t_k) - u_c(t_k)) + \rho \quad (14)
$$

where $x_e(t_k) = -\tilde{A}^{-1}(B_R r(t_k) + \bar{B}_R r(t_k - h_0))$ and $u_c(t_k) = \tilde{K}x_e(t_k) + K_R r(t_k) + \bar{K}_R r(t_k - h_0)$. Note that $\tilde{A}$ is invertible when $\Psi < 0$ (Lemma 3.2). The controller updates the signal according to

$$
\tilde{u}(t) = \begin{cases} u(t_k), \ t \in [t_k, t_{k+1}), & \text{if (14) is true,} \\ \tilde{u}(t_{k-1}), \ t \in [t_k, t_{k+1}), & \text{if (14) is false,} \end{cases} \quad (15)
$$

with $\tilde{u}_0 = u(t_0)$.

Remark 3.2: The modified event trigger (14)–(15) extends the trigger (8)–(9), by including a steady-state control signal term.

Theorem 3.2: *Consider the closed-loop system* (12) *with $d(t) \equiv 0$ and the event trigger* (14)–(15) *with $\rho = 0$. Assume that there exist $P, W_0, W_i, \bar{W}_i, Q_i, R_i \in \mathbb{S}_{++}^n, i \in \mathcal{N}$, $w > 0$, $\sigma > 0$, and $\alpha > 0$, such that $\Psi < 0$. Then the equilibrium point $x_e^* \triangleq -\tilde{A}^{-1}(B_R + \bar{B}_R)r$ is exponentially stable with decay rate α.*

Proof: By Lemma 3.2, there exists an equilibrium point x_e^*. We apply a coordinate transformation $\bar{x}(t) = x(t) - x_e^*$. Then the system (12) can be written as

$$
\dot{\bar{x}}(t) = A\bar{x}(t) + A_0\bar{x}(t_k) + \sum_{i\in\mathcal{N}}A_i\bar{x}(s_i(t_k))
$$
$$
+ \sum_{i\in\mathcal{N}}\bar{A}_i\bar{x}(s_i(t_k) - h_i) + B\xi(t).
$$

By Theorem 3.1, this system is exponentially stable with the event-triggering condition

$$
(\bar{u}(t_k) - \tilde{\bar{u}}(t_{k-1}))^{\top}\Omega(\bar{u}(t_k) - \tilde{\bar{u}}(t_{k-1})) > \sigma\bar{u}^{\top}(t_k)\Omega\bar{u}(t_k)
$$

where $\bar{u}(t_k) = u(t_k) - u_c(t_k)$ and

$$
\tilde{\bar{u}}(t) = \begin{cases} \bar{u}(t_k), \ t \in [t_k, t_{k+1}), & \text{if (14) is true,} \\ \tilde{\bar{u}}(t_{k-1}), \ t \in [t_k, t_{k+1}), & \text{if (14) is false,} \end{cases}
$$

Recall that $r(t)$ is a step function, we have

$$\bar{u}(t_k) - \tilde{u}(t_{k-1})) = u(t_k) - u_c(t_k) - \tilde{u}(t_{k-1}) + u_c(t_{k-1})$$
$$= u(t_k) - \tilde{u}(t_{k-1}).$$

This completes the proof. ∎

Next, we consider disturbance rejection. We introduce an observer to estimate the steady-state control signal, which cannot be obtained when there is an unknown disturbance. The block diagram of the proposed system is shown in Figure 3. In this system, the disturbance estimation $\hat{d}(t_k)$ is used in the controller for feedforward compensation. To model this system, consider the augmented plant

$$\dot{x}_a(t) = A_a x_a(t) + B_a \tilde{u}(t), \tag{16}$$
$$y_i(t) = C_a^i x_a(t), \quad i \in \mathcal{N}, \tag{17}$$

where $x_a(t) = [x_p^\top(t), d^\top]^\top \in \mathbb{R}^{n_p + n_d}$ with

$$A_a = \begin{bmatrix} A_p & B_d \\ 0 & 0 \end{bmatrix}, \quad B_a = \begin{bmatrix} B_p \\ 0 \end{bmatrix}, \quad C_a^i = \begin{bmatrix} C_p^i & 0 \end{bmatrix}.$$

For the system (16)–(17), we introduce an observer with sampled-data implementation

$$\dot{\hat{x}}_a(t) = A_a \hat{x}_a(t_k) + B_a \tilde{u}(t) + \sum_{i \in \mathcal{N}} L_i(y_i(s_i(t_k)) - L C_a \hat{x}(t_k)) \tag{18}$$

where $\hat{x}_a(t) = [\hat{x}_p^\top(t), \hat{d}^\top(t)]^\top$ is the estimate of $x_a(t)$, $L_i = [L_p^{i\top}, L_d^{i\top}]^\top \in \mathbb{R}^{n_p + n_d}$, $L = [L_1, \dots, L_N]$, the observer gain, and $C_a = [C_a^{1\top}, \dots, C_a^{N\top}]^\top$. Introducing $e_p(t) \triangleq x_p(t) - \hat{x}_p(t)$, $e_d(t) \triangleq d - \hat{d}(t)$, and

$$H_p^i \triangleq L_p^i C_p^i, \quad \bar{H}_p \triangleq \sum_{i \in \mathcal{N}} H_p^i, \quad H_d^i \triangleq L_d^i C_p^i, \quad \bar{H}_d \triangleq \sum_{i \in \mathcal{N}} H_d^i,$$

we have the plant state estimation error dynamics

$$\dot{e}_p(t) = A_p x_p(t) - \left(A_p - \bar{H}_p\right) x_p(t_k)$$
$$- \sum_{i \in \mathcal{N}} H_p^i x_p(s_i(t_k)) + A_p e_p(t_k) + B_d e_d(t_k),$$

and the disturbance estimation error dynamics

$$\dot{e}_d(t) = -\bar{H}_d x_p(t_k) - \sum_{i \in \mathcal{N}} H_p^i x_p(s_i(t_k)) + \bar{H}_d e_p(t_k).$$

This gives the controller

$$\dot{x}_c(t) = A_c x_c(t_k) + \sum_{i \in \mathcal{N}} B_c^i y_i(s_i(t_k)) + \sum_{i \in \mathcal{N}} \bar{B}_c^i y_i(s_i(t_k) - h_i)$$
$$+ B_r r(t) + \bar{B}_r r(t_k - h_0) + B_{\hat{d}} \hat{d}(t_k), \tag{19}$$

$$u(t) = C_c x_c(t_k) + \sum_{i \in \mathcal{N}} D_c^i y_i(s_i(t_k)) + \sum_{i \in \mathcal{N}} \bar{D}_c^i y_i(s_i(t_k) - h_i)$$
$$+ D_r r(t_k) + \bar{D}_r r(t_k - h_0) + D_{\hat{d}} \hat{d}(t_k). \tag{20}$$

By augmenting the state

$$\mathbf{x}(t) \triangleq \begin{bmatrix} x_p(t) \\ x_c(t) \\ e_p(t) \\ e_d(t) \end{bmatrix} \in \mathbb{R}^{n + n_p + n_d},$$

we have the following closed-loop system description

$$\dot{\mathbf{x}}(t) = \mathbf{A}\mathbf{x}(t) + \mathbf{A}_0 \mathbf{x}(t_k) + \sum_{i \in \mathcal{N}} \mathbf{A}_i \mathbf{x}(s_i(t_k))$$
$$+ \sum_{i \in \mathcal{N}} \bar{\mathbf{A}}_i \mathbf{x}(s_i(t_k) - h_i)$$
$$+ \mathbf{B}\xi(t) + \mathbf{B}_D d(t) + \mathbf{B}_R r(t_k) + \bar{\mathbf{B}}_R r(t_k - h_0) \tag{21}$$

with

$$\mathbf{A} = \begin{bmatrix} A_p & 0 & 0 & 0 \\ 0 & 0 & 0 & 0 \\ A_p & 0 & 0 & 0 \\ 0 & 0 & 0 & 0 \end{bmatrix},$$

$$\mathbf{A}_0 = \begin{bmatrix} 0 & B_p C_c & 0 & -B_p D_{\hat{d}} \\ 0 & A_c & 0 & -B_{\hat{d}} \\ -A_p + \bar{H}_p & 0 & A_p & B_d \\ \bar{H}_d & 0 & -\bar{H}_d & 0 \end{bmatrix},$$

$$\mathbf{A}_i = \begin{bmatrix} B_p D_c^i C_p^i & 0 & 0 & 0 \\ B_c^i C_p^i & 0 & 0 & 0 \\ -H_p^i & 0 & 0 & 0 \\ -H_d^i & 0 & 0 & 0 \end{bmatrix},$$

$$\bar{\mathbf{A}}_i = \begin{bmatrix} B_p \bar{D}_c^i C_p^i & 0 & 0 & 0 \\ \bar{B}_c^i C_p^i & 0 & 0 & 0 \\ 0 & 0 & 0 & 0 \\ 0 & 0 & 0 & 0 \end{bmatrix}, \quad \mathbf{B} = \begin{bmatrix} B_p \\ 0 \\ 0 \\ 0 \end{bmatrix},$$

$$\mathbf{B}_D = \begin{bmatrix} B_d + B_p D_{\hat{d}} \\ B_{\hat{d}} \\ 0 \\ 0 \end{bmatrix}, \quad \mathbf{B}_R = \begin{bmatrix} B_p D_r \\ B_r \\ 0 \\ 0 \end{bmatrix}, \quad \bar{\mathbf{B}}_R = \begin{bmatrix} B_p \bar{D}_r \\ \bar{B}_r \\ 0 \\ 0 \end{bmatrix}.$$

Similar to (12), let us denote

$$\bar{\mathbf{A}} \triangleq \mathbf{A} + \mathbf{A}_0 + \sum_{i \in \mathcal{N}} \mathbf{A}_i, \quad \tilde{\mathbf{A}} \triangleq \bar{\mathbf{A}} + \sum_{i \in \mathcal{N}} \bar{\mathbf{A}}_i,$$

$$\mathbf{K}_0 \triangleq \begin{bmatrix} 0 & C_c & 0 & 0 \end{bmatrix}, \quad \mathbf{K}_i = \begin{bmatrix} D_c^i C_p^i & 0 & 0 & 0 \end{bmatrix},$$

$$\bar{\mathbf{K}}_i \triangleq \begin{bmatrix} \bar{D}_c^i C_p^i & 0 & 0 & 0 \end{bmatrix}, \quad \bar{\mathbf{K}} \triangleq \mathbf{K}_0 + \sum_{i \in \mathcal{N}} \mathbf{K}_i,$$

$$\tilde{\mathbf{K}} \triangleq \bar{\mathbf{K}} + \sum_{i \in \mathcal{N}} \bar{\mathbf{K}}_i, \quad \mathbf{K}_R \triangleq D_r, \quad \bar{\mathbf{K}}_R \triangleq \bar{D}_r, \quad \mathbf{K}_D \triangleq D_{\hat{d}}.$$

We now consider the event-triggering condition

$$(u(t_k) - \tilde{u}(t_{k-1}))^\top \Omega (u(t_k) - \tilde{u}(t_{k-1}))$$
$$> \sigma (u(t_k) - \mathbf{u}_c(t_k))^\top \Omega (u(t_k) - \mathbf{u}_c(t_k)) + \rho \tag{22}$$
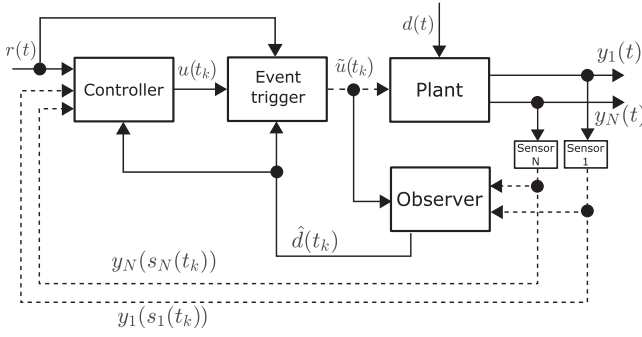
Figure 3. Block diagram of the event-triggered control system for setpoint tracking and disturbance rejection.

where

$$\mathbf{x}_e(t_k) \triangleq -\tilde{\mathbf{A}}^{-1}(\mathbf{B}_D \hat{d}(t_k) + \mathbf{B}_R r(t_k) + \bar{\mathbf{B}}_R r(t_k - h_0))$$

and

$$\mathbf{u}_c(t_k) = \tilde{\mathbf{K}}\mathbf{x}_e(t_k) + \mathbf{K}_R r(t_k) + \bar{\mathbf{K}}_R r(t_k - h_0) + \mathbf{K}_D \hat{d}(t_k).$$

Under this condition, the controller updates its signal according to

$$\tilde{u}(t) = \begin{cases} u(t_k), \ t \in [t_k, t_{k+1}), & \text{if (22) is true,} \\ \tilde{u}(t_{k-1}), \quad t \in [t_k, t_{k+1}), & \text{if (22) is false,} \end{cases} \quad (23)$$

with $\tilde{u}_0 = u(t_0)$. This event-triggered control systems is exponentially stable, as stated next.

Theorem 3.3: *Consider the closed-loop system* (21) *and the event trigger* (22)–(23) *with* $\rho = 0$. *Assume that there exist* $P, W_0, W_i, Q_i, R_i \in \mathbb{S}^{n+n_p+n_d}$, $w > 0$, $\sigma > 0$, *and* $\alpha > 0$, *such that* $\Xi = \Xi^\top = \{\Xi_{j\ell}\} < 0$ *where*

$$\Xi_{11} = P\bar{A} + \bar{A}^\top P + 2\alpha P + \sum_{i \in \mathcal{N}}\left[Q_i - e^{-2\alpha h_i} R_i\right],$$

$$\Xi_{1(i+1)} = P\bar{A}_i + e^{-2\alpha h_i} R_i, \quad i = 1, \ldots, N,$$

$$\Xi_{1(i+N+2)} = PA_i, \quad i = 0, 1, \ldots, N,$$

$$\Xi_{1(i+2N+2)} = P\bar{A}_i, \quad i = 1, \ldots, N,$$

$$\Xi_{1(3N+3)} = \bar{A}^\top S, \quad \Xi_{1(3N+4)} = PB, \quad \Xi_{1(3N+5)} = w\sigma F^\top \Omega,$$

$$\Xi_{(i+1)(i+1)} = -e^{-2\alpha h_i}(Q_i + R_i), \quad i = 1, \ldots, N,$$

$$\Xi_{(i+1)(3N+3)} = \bar{A}_i^\top S, \quad i = 1, \ldots, N,$$

$$\Xi_{(i+1)(3N+5)} = w\sigma \bar{K}_i^\top \Omega, \quad i = 1, \ldots, N,$$

$$\Xi_{(i+N+2)(i+N+2)} = -\frac{\pi^2}{4} W_i, \quad i = 0, 1, \ldots, N,$$

$$\Xi_{(i+N+2)(3N+3)} = A_i^\top S, \quad i = 0, 1, \ldots, N,$$

$$\Xi_{(N+2)(3N+5)} = w\sigma F_0^\top \Omega,$$

$$\Xi_{(i+N+2)(3N+5)} = w\sigma K_i^\top \Omega, \quad i = 1, \ldots, N,$$

$$\Xi_{(i+2N+2)(i+2N+2)} = -\frac{\pi^2}{4} e^{-2\alpha h_i} \bar{W}_i, \quad i = 1, \ldots, N,$$

$$\Xi_{(i+2N+2)(3N+3)} = \bar{A}_i^\top S, \quad i = 1, \ldots, N,$$

$$\Xi_{(i+2N+2)(3N+5)} = w\sigma \bar{K}_i^\top \Omega, \quad i = 1, \ldots, N,$$

$$\Xi_{(3N+3)(3N+3)} = -S, \quad \Xi_{(3N+3)(3N+4)} = SB,$$

$$\Xi_{(3N+4)(3N+4)} = -w\Omega, \quad \Xi_{(3N+5)(3N+5)} = -w\sigma \Omega,$$

with

$$S \triangleq h_0^2 e^{-2\alpha h_0} W_0$$
$$+ \sum_{i \in \mathcal{N}}\left[(h_0 + h_i)^2 e^{-2\alpha(h_0+h_i)}(W_i + \bar{W}_i) + h_i^2 R_i\right],$$

$F_0 \triangleq K_0 - \tilde{K}\tilde{A}^{-1} B_D E$, $F \triangleq \bar{K} - \tilde{K}\tilde{A}^{-1} B_D E$ *with* $E \triangleq [0 \ \ 0 \ \ 0 \ \ I_{n_d}]$, *and the other elements are zero matrices. Then the equilibrium point* $x_e^* \triangleq -\tilde{A}^{-1}(B_D d + (B_R + \bar{B}_R)r)$ *is exponentially stable with decay rate* α.

Proof: See Appendix 3. ∎

In virtue of Theorem 3.3, we can obtain the optimal threshold σ^* for a given convergence rate α.

Corollary 3.1: *Given* $w > 0$ *and* $\alpha > 0$, *if the SDP*

$$\sigma^* \triangleq \max \sigma \quad \text{s.t. } \Xi < 0 \quad (24)$$

is feasible, then the closed-loop system (21) *with the event trigger* (22)–(23) *with* $\sigma = \sigma^*$ *is exponentially stable with decay rate* α.

Proof: If the SDP (24) is feasible, we have $\Xi < 0$. Then by Theorem 3.3, the system (21) with the event trigger (22)–(23) with $\sigma = \sigma^*$ is exponentially stable with decay rate α. ∎

Remark 3.3: If only setpoint tracking is considered, the observer is not needed. The constraint $\Xi < 0$ in (24) is then simplified to $\Phi < 0$.

Remark 3.4: The outcome of the SDP (24) may severely depend on the choice of w. To find the maximum threshold σ^* with respect to w, one should solve the SDP (24) repeatedly with different values of $w \geq 0$.

4. Applications to PID, cascade, and decoupling control

In this section, we apply the theoretical results of the previous section to PID, cascade, and decoupling control. Numerical examples are also provided to illustrate how the proposed controllers and event thresholds are obtained.

4.1 PI and PID control

First, we apply the results to PI control. A PI controller is given by (19)–(20) with $A_c = 0$, $B_c^1 = -1$, $\bar{B}_c^1 = 0$, $B_r = 1$, $\bar{B}_r = 0$, $B_{\hat{d}} = 0$, $C_c = K_i$, $D_c^1 = -K_p$, $\bar{D}_c^1 = 0$, $D_r = K_p$, $\bar{D}_r = 0$, and $D_{\hat{d}} = K_f$, where K_f is the feedforward gain. By setting the control parameters K_p, K_i, K_f, sampling intervals h_0, h_1 in (3)–(4),

Table 1. Comparison of the ETC, PIDPLUS, SOD, and TTC.

Type	IAE	# events until $t = 500$
ETC	19.5	47
PIDPLUS	34.7	73
SOD	44.0	96
TTC	27.7	1667

decay rate α, and observer gain L, the maximum threshold is obtained by solving SDP (24).

Example 4.1: We first illustrate an example of PI control for a first-order linear system and compare the proposed event-triggered control (ETC) with three different strategies: event-triggered PIDPLUS control (PIDPLUS, Tiberi et al. (2012)), event-triggered PI control with send-on-delta triggering (SOD, Kiener et al. (2014)), and time-triggered control (TTC). We assume that all the controllers are co-located at the sensor since the event-triggered PIDPLUS control needs to have the controller capability at the sensor.

Consider a first-order linear system

$$\dot{x}_p(t) = -0.7x_p(t) + \tilde{u}(t) + d(t) + w(t),$$
$$y(t) = x_p(t),$$

where $w(t) \in \mathbb{R}$ is the random process noise, which is assumed to be Gaussian with zero-mean independent and identically distributed with variance 0.25. The control parameters are given with $K_{\mathrm{p}} = 0.23$, $K_{\mathrm{i}} = 0.077$, and $K_{\mathrm{f}} = -0.5$. The sampling intervals are set with $h_0 = h_1 = 0.3$ using the criteria in Åström and Wittenmark (2013). By solving SDP (24), we obtain $\sigma^* = 2.72$. The SDP can be effectively solved by YALMIP toolbox (Löfberg, 2004). We consider the reference signal $r(t) = 1, \forall t \geq 0$ and the disturbance $d(t) = -0.5, \forall t \geq 250$. The response with $\rho = 10^{-5}$ is shown in Figure 4 together with PIDPLUS, SOD, and TTC.

To evaluate the performances, we introduce the Integral of the Absolute Error (IAE) as

$$\text{IAE} = \int_0^{t_f} |r(t) - y_1(t)| \, dt \tag{25}$$

with $t_f = 500$. The IAEs and the numbers of event generations (the average of 1000 times simulations) are shown in Table 1. It can be found that the ETC extremely reduces communications compared with the TTC while both controllers update each state every $h = 0.3$ seconds. The ETC achieves smaller IAE than the PIDPLUS and SOD with less samples. This is partially because observer-based feedforward control is employed in the ETC.

Next, we consider PID control. Setting PID control parameters K_{p}, K_{i}, K_{d}, T_1, K_{f}, and sampling intervals h_0, h_1 in (5)–(7), a PID controller can be written as the form (19)–(20) with

$$A_c = \begin{bmatrix} 0 & 0 \\ 0 & -1/T_1 \end{bmatrix}, \quad B_c^1 = \begin{bmatrix} -1 \\ -1/T_1 h_1 \end{bmatrix},$$
$$\bar{B}_c^1 = \begin{bmatrix} 0 \\ 1/T_1 h_1 \end{bmatrix}, \quad B_r = \begin{bmatrix} 1 \\ c/T_1 h_0 \end{bmatrix},$$
$$\bar{B}_r = \begin{bmatrix} 0 \\ -c/T_1 h_0 \end{bmatrix}, \quad B_{\hat{d}} = \begin{bmatrix} 0 \\ 0 \end{bmatrix},$$

Table 2. Obtained thresholds for the PID (including PI-D and I-PD) control with and without FF.

	PID	PID+FF
σ^*	0.19	0.40

Table 3. Comparison of the ETCs and TTCs.

Type	T_r	M	T_s	IAE	# events untill T_s
ETC (PID)	0.51	6.4	2.80	1.34	21
ETC (PID+FF)	0.49	5.8	2.73	0.94	16
TTC (PID)	0.53	7.7	3.04	1.37	299
ETC (PI-D)	0.59	11.1	2.98	1.46	18
ETC (PI-D+FF)	0.59	11.4	2.96	1.07	14
TTC (PI-D)	0.56	9.1	3.08	1.40	303
ETC (I-PD)	1.15	4.5	3.54	1.90	31
ETC (I-PD+FF)	1.18	4.6	3.41	1.50	25
TTC (I-PD)	1.14	3.3	3.54	1.85	340

$$C_c = \begin{bmatrix} K_{\mathrm{i}} & K_{\mathrm{d}} \end{bmatrix}, \quad D_c^1 = -K_{\mathrm{p}}, \quad \bar{D}_c^1 = 0,$$
$$D_r = bK_{\mathrm{p}}, \quad \bar{D}_r = 0, \quad D_{\hat{d}} = K_{\mathrm{f}}.$$

Note that PID controllers have variations based on settings of weight parameters b and c. We indicate the case $b = c = 1$ by PID, $b = 1$, $c = 0$ by PI-D, and $b = c = 0$ by I-PD. Setting decay rate α and observer gain L, the maximum threshold σ^* is obtained by solving SDP (24).

Example 4.2: Consider a linear system

$$\dot{x}_p(t) = \begin{bmatrix} -1 & 1 \\ 0 & -10 \end{bmatrix} x_p(t) + \begin{bmatrix} 0 \\ 4 \end{bmatrix} (\tilde{u}(t) + d(t)),$$
$$y(t) = \begin{bmatrix} 2.5 & 0 \end{bmatrix} x_p(t),$$

and PID, PI-D, and I-PD controllers with the parameters: $K_{\mathrm{p}} = 1.63, K_{\mathrm{i}} = 2.71, K_{\mathrm{d}} = 0.075$, and $T_1 = 0.052$. The control parameters are obtained by applying MATLAB function pidtune. By solving SDPs (24) with intervals $h_0 = h_1 = 0.01$ and $\alpha = 0.3$ for the two cases: PID both with and without feedforward controller (FF, $K_{\mathrm{f}} = -0.5$), we find the event thresholds as in Table 2.

We consider the reference signal $r(t) = 1, \forall t \geq 0$ and disturbance $d(t) = -2, \forall t \geq 10$. Numerical results with $\rho = 10^{-5}$ for ETC with and without FF, compared to TTC, are shown in Figure 5 and Table 3.

As performance metrics, we introduce the rise time T_r [1], overshoot M [2], settling time T_s [3], and the IAE (25) with $t_f = 20$. It can be found from Figure 5 that the ETCs compensate for the step disturbances as we showed in Theorem 3.3. Thanks to feedforward controllers, the effects of the disturbances are reduced more efficiently. The IAEs of the ETCs with FF are smaller than those of the ETCs without FF and TTCs as in Table 3. The response of each ETC (blue solid line) are similar to the TTC (orange dash-dotted line) in Figure 5. We can see that the event-triggered controllers can track their setpoints as well as the time-triggered controllers without performance degradation. In fact, the quantities such as rise time, overshoot, and settling time for the ETCs and TTCs are almost same (Table 3). We also indicate the number of event generations until $t = T_s$. It can be seen that event generations are extremely reduced compared to the TTCs while keeping the control performance.
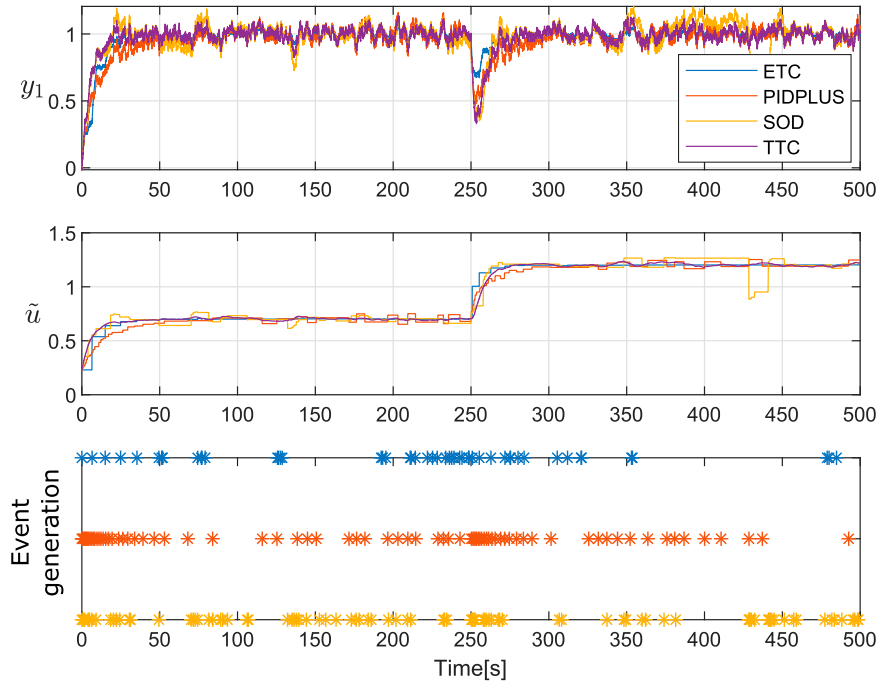
Figure 4. Responses of the proposed event-triggered PI control (ETC, blue), PIDPLUS (red), SOD (orange), and TTC (purple). The top plot describes the outputs, the middle control signals, and the bottom event generations.

4.2 Cascade control

With given control and sampling parameters, a cascade controller (19)–(20) is given by

$$A_c = \begin{bmatrix} 0 & 0 & 0 & 0 \\ 0 & -1/T_1 & 0 & 0 \\ K_i^1 & K_d^1 & 0 & 0 \\ 0 & 0 & 0 & -1/T_2 \end{bmatrix},$$

$$B_c^1 = \begin{bmatrix} -1 \\ -1/T_1 h_1 \\ -K_p^1 \\ 0 \end{bmatrix}, \quad B_c^2 = \begin{bmatrix} 0 \\ 0 \\ -1 \\ -1/T_2 h_2 \end{bmatrix},$$

$$\bar{B}_c^1 = \begin{bmatrix} 0 \\ 1/T_1 h_1 \\ 0 \\ 0 \end{bmatrix}, \quad \bar{B}_c^2 = \begin{bmatrix} 0 \\ 0 \\ 0 \\ 1/T_2 h_2 \end{bmatrix}, \quad B_r = \begin{bmatrix} 1 \\ c/T_1 h_0 \\ bK_p^1 \\ 0 \end{bmatrix},$$

$$\bar{B}_r = \begin{bmatrix} 0 \\ -c/T_1 h_0 \\ 0 \\ 0 \end{bmatrix}, \quad B_{\hat{d}} = \begin{bmatrix} 0 \\ 0 \\ 0 \\ K_f \end{bmatrix},$$

$$C_c = \begin{bmatrix} K_p^2 K_i^1 & K_p^2 K_d^1 & K_i^2 & K_d^2 \end{bmatrix}, \quad D_c^1 = -K_p^1 K_p^2,$$

$$D_c^2 = -K_p^2, \bar{D}_c^1 = 0, \quad \bar{D}_c^2 = 0, D_r = bK_p^1 K_p^2,$$

$$\bar{D}_r = 0, \quad D_{\hat{d}} = K_p^2 K_f.$$

The block diagram of event-triggered cascade control with an observer is shown in Figure 6.

Example 4.3: Consider the system illustrated by Figure 6, where plant 1 is given by

$$\dot{x}_{p,1}(t) = \begin{bmatrix} -1 & 1 & 0 \\ 0 & -1.2 & 1 \\ 0 & 0 & -1.5 \end{bmatrix} x_{p,1}(t) + \begin{bmatrix} 0 \\ 0 \\ 4 \end{bmatrix} y_2(t),$$

$$y_1(t) = \begin{bmatrix} 2.5 & 0 & 0 \end{bmatrix} x_{p,1}(t),$$

and plant 2 by

$$\dot{x}_{p,2}(t) = -2x_{p,2}(t) + 2\left(\tilde{u}(t) + d(t)\right),$$

$$y_2(t) = 1.5x_{p,2}(t).$$

We apply event-triggered cascade control (CAS) with a PID–PI pair: $K_p^1 = 0.18, K_i^1 = 0.0791, K_d^1 = 0.0439, T_1 = 0.0175$ for the outer controller and $K_p^2 = 0.244, K_i^2 = 1.82$ for the inner controller, with and without feedforward control $K_f = -0.5$. We compare this to PI control with $K_p = 0.109, K_i = 0.0488$. Solving SDPs (24) with intervals $h_0 = 0.02, h_1 = 0.04, h_2 = 0.02$, and $\alpha = 0.1$, the event thresholds are obtained as summarized in Table 4.

We consider the disturbance signal $d(t) = 0.05, \forall t \geq 0$. Numerical results with $\rho = 10^{-8}$ are shown in Figure 7 and Table 5. It can be found from Figure 7 that the proposed event-triggered cascade controller compensates for the disturbance. Compared to the event-triggered PI control, the effect of the disturbance is significantly reduced. The maximum value of output $y_1(t)$ is about 0.05 (without FF), while that of the PI control is more than 0.25. The IAE of the cascade control are around 0.3, while that of the PI control are around 1.0. We can also see that the disturbances are effectively compensated by the feedforward control in both cascade and PI controllers. We indicate the number of event generations of each event-triggered
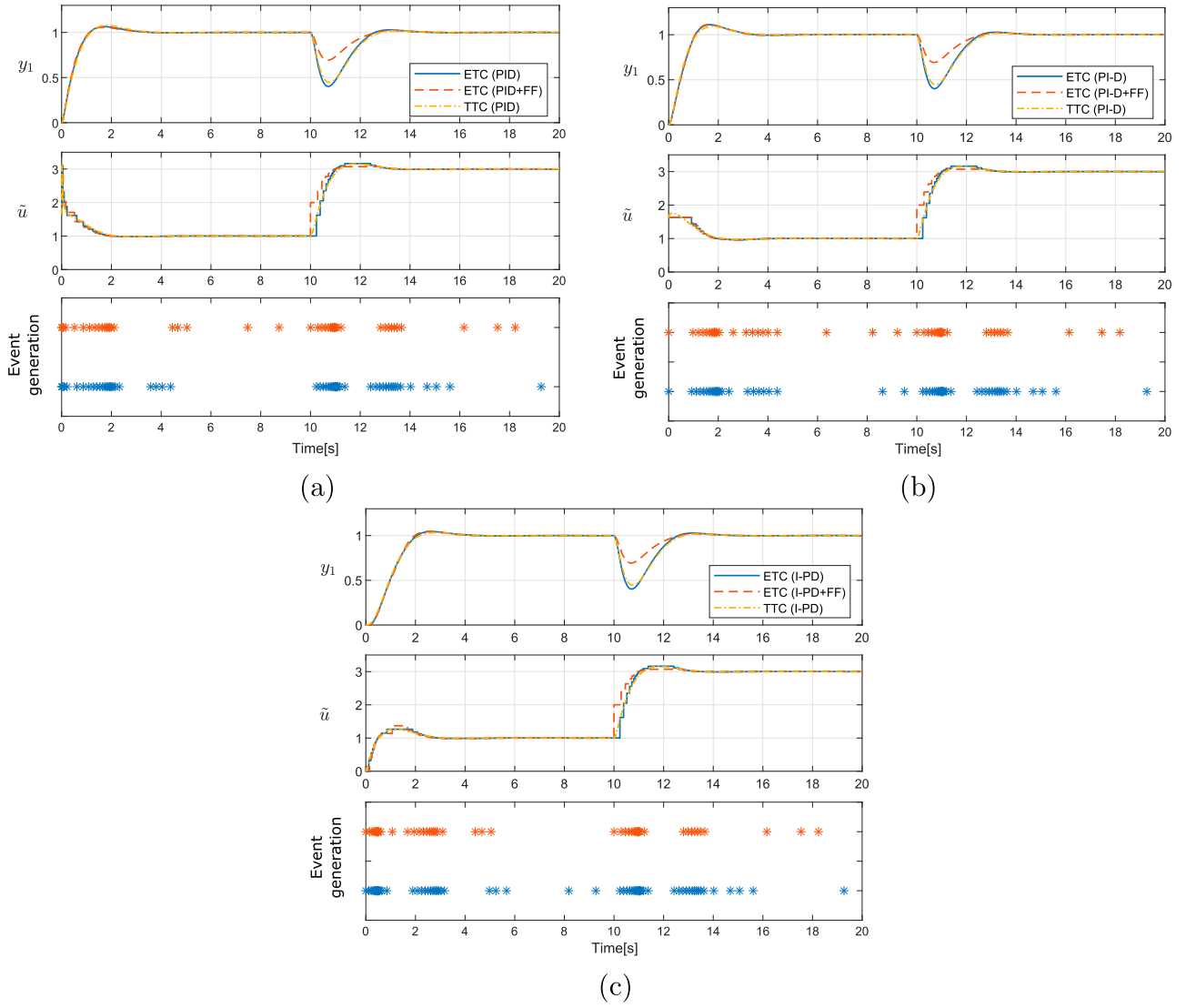
Figure 5. Responses of the event-triggered control (ETC without FF: blue, with FF: red) and the time-triggered control (TTC: orange). In each figure, three plots show the outputs, control signals, and event generations of the ETCs from the top. (a) PID control (b) PI-D control (c) I-PD control.

Table 4. Obtained thresholds for the cascade and PI control.

	CAS	CAS+FF	PI	PI+FF
σ^*	0.79	0.80	0.07	0.18

Table 5. Numerical results of the event-triggered and time-triggered cascade/PI control.

Type	$y_{1,max}$	IAE	# events untill $t = 20$
ETC (CAS)	0.055	0.296	41
ETC (CAS+FF)	0.027	0.176	32
TTC (CAS)	0.048	0.177	1000
ETC (PI)	0.257	1.058	73
ETC (PI+FF)	0.132	0.547	65
TTC (PI)	0.241	1.025	1000

controller until $t = 20$ in Table 5. It can be seen that event generations are extremely reduced compared to the time-triggered cascacde control with slight performance degradation, which can be further reduced by introducing feedfoward control.
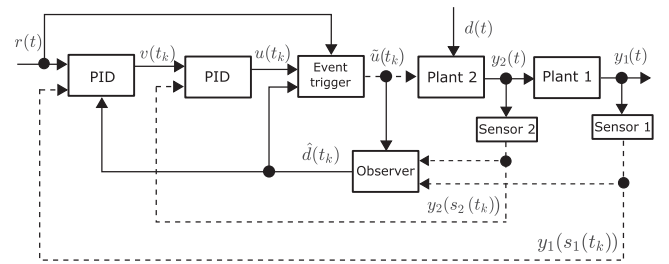
Figure 6. Event-triggered cascade control with an observer.

4.3 Decoupling control

A decoupling controller can be written by the form of (19)–(20) with

$$A_c = \begin{bmatrix} 0 & 0 & 0 & 0 \\ 0 & -1/T_1 & 0 & 0 \\ 0 & 0 & 0 & 0 \\ 0 & 0 & 0 & -1/T_2 \end{bmatrix}, \quad B_c^1 = \begin{bmatrix} -1 \\ -c_1/T_1 h_1 \\ 0 \\ 0 \end{bmatrix},$$
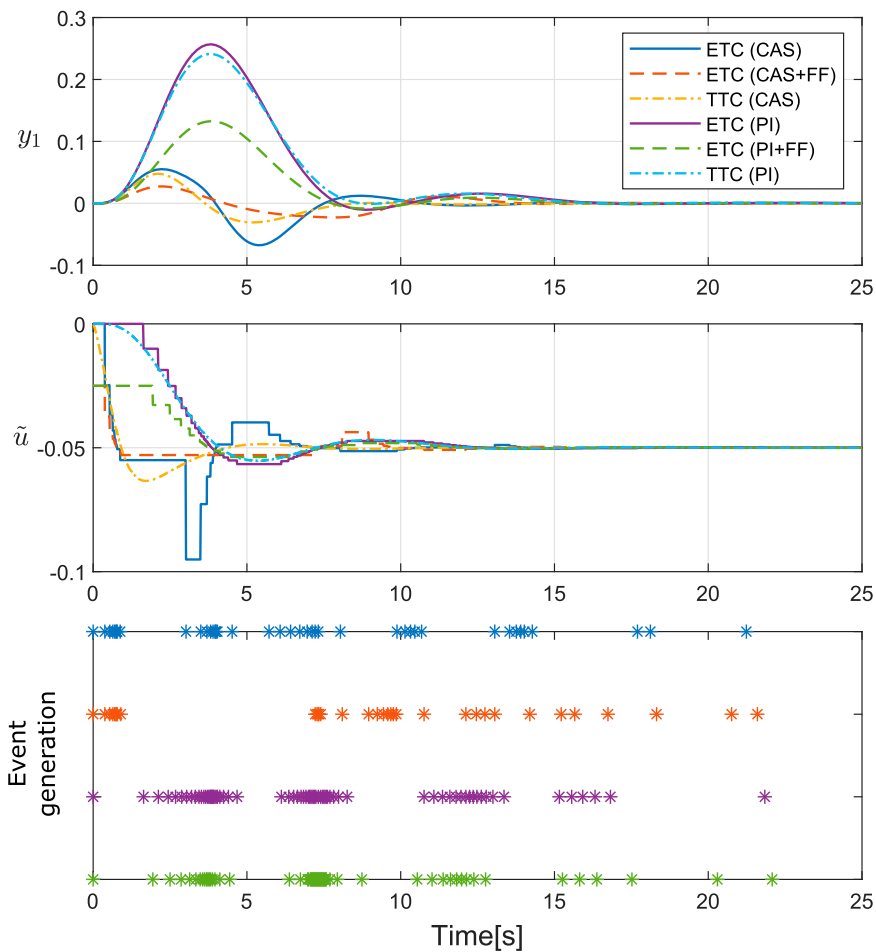
Figure 7. Responses of the event-triggered cascade control (ETC (CAS)), time-triggered cascade control (TTC (CAS)), event-triggered PI control (ETC (PI)), and time-triggered PI control (TTC (PI)). The top plot describes the outputs, the middle control signals, and the bottom the event generations of ETCs.
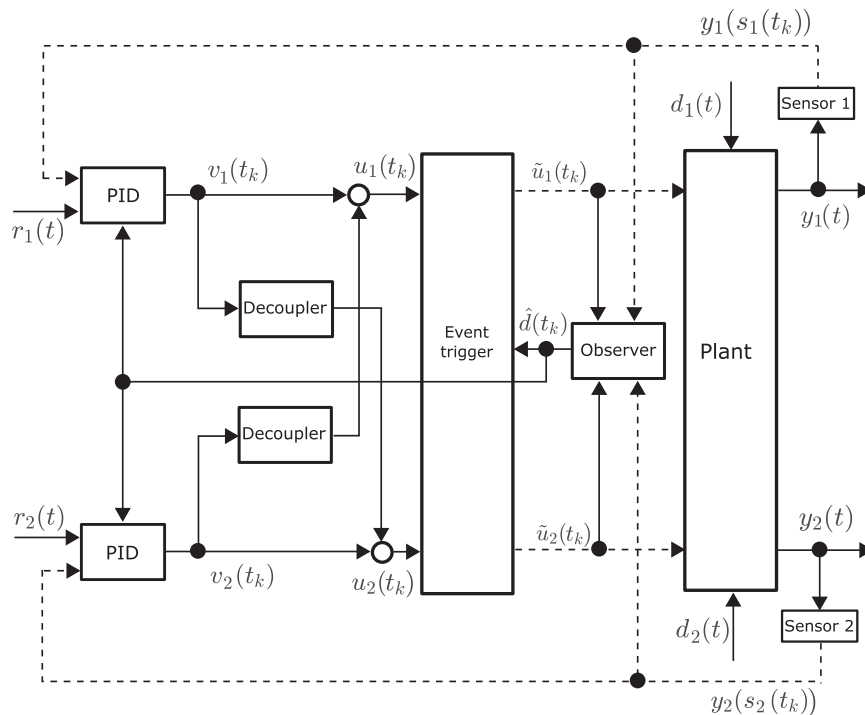

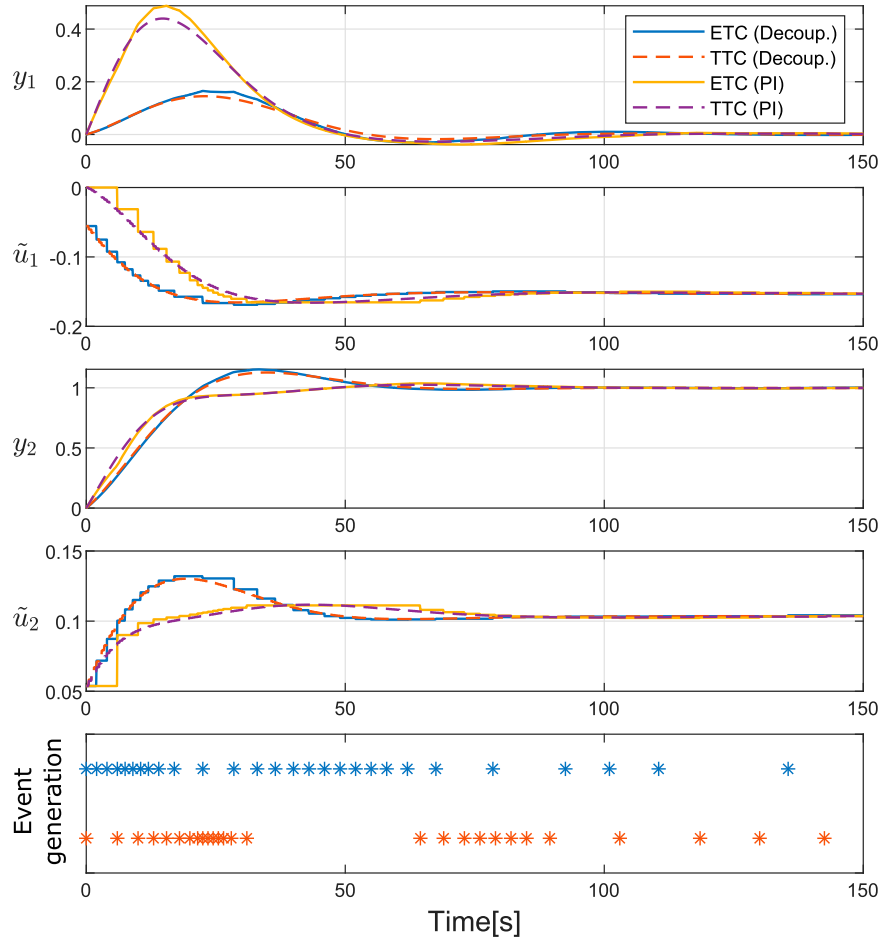**Figure 8.** Event-triggered decoupling control with an observer.

Figure 9. Responses of the event-triggered decoupling control (ETC (Decoup.)), time-triggered decoupling control (TTC (Decoup.)), event-triggered PI control (ETC (PI)), and time-triggered PI control (TTC (PI)). From the top, each plot describes the outputs $y_1(t)$ and control signal $\tilde{u}_1(t)$ of one control loop, outputs $y_2(t)$ and control signal $\tilde{u}_2(t)$ of another, and the event generations of ETCs.

$$B_c^2 = \begin{bmatrix} 0 \\ 0 \\ -1 \\ -c_2/T_2 h_2 \end{bmatrix}, \quad \bar{B}_c^1 = \begin{bmatrix} 0 \\ c_1/T_1 h_1 \\ 0 \\ 0 \end{bmatrix},$$

$$\bar{B}_c^2 = \begin{bmatrix} 0 \\ 0 \\ 0 \\ c_2/T_2 h_2 \end{bmatrix}, \quad B_r = \begin{bmatrix} 1 & 0 \\ c_1/T_1 h_0 & 0 \\ 0 & 1 \\ 0 & c_2/T_2 h_0 \end{bmatrix},$$

$$\bar{B}_r = \begin{bmatrix} 0 & 0 \\ -c_1/T_1 & 0 \\ 0 & 0 \\ 0 & -c_2/T_2 \end{bmatrix},$$

$$C_c = \begin{bmatrix} K_i^1 & K_d^1 & K_g^1 K_i^2 & K_g^1 K_d^2 \\ K_g^2 K_i^1 & K_g^2 K_d^1 & K_i^2 & K_d^2 \end{bmatrix},$$

$$D_c^1 = \begin{bmatrix} -K_p^1 \\ -K_g^2 K_p^1 \end{bmatrix}, \quad D_c^2 = \begin{bmatrix} -K_g^1 K_p^2 \\ -K_p^2 \end{bmatrix}, \quad \bar{D}_c^1 = \bar{D}_c^1 = \begin{bmatrix} 0 \\ 0 \end{bmatrix},$$

$$D_r = \begin{bmatrix} b_1 K_p^1 & b_1 K_g^1 K_p^2 \\ b_2 K_g^2 K_p^1 & b_2 K_p^2 \end{bmatrix}, \quad \bar{D}_r = \begin{bmatrix} 0 & 0 \\ 0 & 0 \end{bmatrix},$$

$$D_d = \begin{bmatrix} K_f^1 & K_g^1 K_f^2 \\ K_g^2 K_f^1 & K_f^2 \end{bmatrix},$$

where K_f^1 and K_f^2 are the feedforward gains of controllers 1 and 2, respectively.

The block diagram of event-triggered decoupling control with an observer is shown in Figure 8.

Example 4.4: Consider the distillation column (Seborg et al., 2010), which state-space formulation is given by

$$\dot{x}_p(t) = \begin{bmatrix} -0.0599 & 0 & 0 & 0 \\ 0 & -0.0476 & 0 & 0 \\ 0 & 0 & -0.0917 & 0 \\ 0 & 0 & 0 & -0.0694 \end{bmatrix} x_p(t)$$

$$+ \begin{bmatrix} 1 & 0 \\ 0 & 1 \\ 1 & 0 \\ 0 & 1 \end{bmatrix} \tilde{u}(t) + \begin{bmatrix} 1 & 0 \\ 0 & 0 \\ 0 & 0 \\ 0 & 1 \end{bmatrix} d(t),$$

$$y_1(t) = \begin{bmatrix} 0.767 & 0.90 & 0 & 0 \end{bmatrix} x_p(t),$$

$$y_2(t) = \begin{bmatrix} 0 & 0 & 0.605 & 1.347 \end{bmatrix} x_p(t).$$

We introduce decoupling control consisting of two PI controllers $K_p^1 = 0.0537, K_i^1 = 0.0112, K_p^2 = 0.0814, K_i^2 = 0.0146$, $K_f^1 = K_f^2 = 0$, and decouplers $[K_g^1, K_g^2] = [-1.0336, -0.2381]$. We compare this to non-decoupled PI control, i.e. $[K_g^1, K_g^2] =$

Table 6. Obtained thresholds for the decoupling control and PI control.

	Decoup.	PI
σ^*	0.097	0.14

Table 7. Numerical results of the event-triggered and time-triggered decoupling/PI control (disturbance rejection).

Type	$y_{1\,max}$	IAE (y_1)
ETC (Decoup.)	0.17	5.56
TTC (Decoup.)	0.15	4.96
ETC (PI)	0.49	13.07
TTC (PI)	0.44	12.26

Table 8. Numerical results of the event-triggered and time-triggered decoupling/PI control (setpoint tracking).

Type	T_r	M	T_s	IAE (y_2)	# events untill T_s
ETC (Decoup.)	12.67	15.4	54.66	14.03	19
TTC (Decoup.)	12.46	12.7	57.42	13.55	115
ETC (PI)	9.89	3.9	80.56	11.06	20
TTC (PI)	9.43	2.5	74.38	10.54	149

$[0, 0]$. By solving SDPs (24) with intervals $h_0 = h_1 = h_2 = 0.5$, and $\alpha = 0.025$, event thresholds are obtained (Table 6).

We consider the step reference signal $r(t) = [0, 1]^\top, \forall t \geq 0$. Numerical results with $\rho = 10^{-6}$ are shown in Figure 9, Tables 7, and 8. It can be found from Figure 9 and Table 7 that the proposed event-triggered decoupling controller compensates well for the disturbance. The number of events until the settling time of $y_2(t)$ is extremely reduced compared to the time-triggered decoupling control with slight performance degradation as shown in Table 8.

5. Conclusion

This paper studied periodic event-triggered PID, cascade, and decoupling control. The controllers update their commands when the values went beyond given thresholds. We formulated an output feedback control system as a general form of the three systems, and derived an exponential stability condition. Furthermore, it was shown that the proposed controller has a capability of setpoint tracking and disturbance rejection. Event threshold tuning was also proposed. We then applied the framework to PI, PID, cascade, and decoupling control. The numerical examples showed that the proposed controllers reduced the communication load while maintaining the control performance. Future work will focus on the experimental validation of the proposed controllers.

Notes

1. Time that the step response $y_1(t)$ takes to rise from 10% to 90%.
2. Percentage overshoot compared to the setpoint.
3. Time that error $|r - y(t)|$ to fall with in 2% of the setpoint.

Disclosure statement

No potential conflict of interest was reported by the author(s).

ORCID

Takuya Iwaki 🔾 http://orcid.org/0000-0001-6809-6035
Emilia Fridman 🔾 http://orcid.org/0000-0002-8773-9494
Karl Henrik Johansson 🔾 http://orcid.org/0000-0001-9940-5929

References

Ahlén, A., Åkerberg, J., Eriksson, M., Isaksson, A. J., Iwaki, T., Johansson, K. H., Knorn, S., Lindh, T., & Sandberg, H. (2019). Toward wireless control in industrial process automation: A case study at a paper mill. *IEEE Control Systems Magazine*, *39*(5), 36–57. https://doi.org/10.1109/MCS.2019.2925226

Araújo, J., Mazo, M., Anta, A., Tabuada, P., & Johansson, K. H. (2014). System architectures, protocols and algorithms for aperiodic wireless control systems. *IEEE Transactions on Industrial Informatics*, *10*(1), 175–184. https://doi.org/10.1109/TII.2013.2262281

Årzén, K. E. (1999). A simple event-based PID controller. In *Proceedings of IFAC world congress* (Vol. 18, pp. 423–428). Elsevier.

Åström, K. J., & Bernhardsson, B. (1999). Comparison of periodic and event based sampling for first-order stochastic systems. In *Proceedings of IFAC world congress* (Vol. 11, pp. 301–306). Elsevier.

Åström, K. J., & Hägglund, T. (2006). *Advanced PID control*. International Society of Automation.

Åström, K. J., & Wittenmark, B. (2013). *Computer-controlled systems: Theory and design*. Prentice-Hall.

Blevins, T., Chen, D., Nixon, M., & Wojsznis, W. (2015). *Wireless control foundation: Continuous and discrete control for the process industry*. International Society of Automation.

Di Girolamo, G. D., & D'Innocenzo, A. (2019). Codesign of controller, routing and scheduling in WirelessHART networked control systems. *International Journal of Robust and Nonlinear Control*, *29*(7), 2171–2187. https://doi.org/10.1002/rnc.v29.7

Donkers, M. C. F., & Heemels, W. P. M. H. (2012). Output-based event-triggered control with guaranteed $\mathcal{L}_\infty$-gain and improved and decentralized event-triggering output-based event-triggered control with guaranteed $\mathcal{L}_\infty$-gain and improved and decentralized event-triggering. *IEEE Transactions on Automatic Control*, *57*(6), 1362–1376. https://doi.org/10.1109/TAC.2011.2174696

Fridman, E. (2014). Tutorial on lyapunov-based methods for time-delay systems. *European Journal of Control*, *20*(6), 271–283. https://doi.org/10.1016/j.ejcon.2014.10.001

Garcia, E., & Antsaklis, P. J. (2014). Event-triggered output feedback stabilization of networked systems with external disturbance. In *Proceedings of IEEE conference on decision and control* (pp. 3566–3571). IEEE.

HART Communication Foundation (2014). WirelessHart overview.

Heemels, W. P. M. H., & Donkers, M. C. F. (2013). Model-based periodic event-triggered control for linear systems. *Automatica*, *49*(3), 698–711. https://doi.org/10.1016/j.automatica.2012.11.025

Heemels, W. P. M. H., Donkers, M. C. F., & Teel, A. R. (2012). Periodic event-triggered control for linear systems. *IEEE Transactions on Automatic Control*, *58*(4), 847–861. https://doi.org/10.1109/TAC.2012.2220443

Heemels, W. P. M. H., Johansson, K. H., & Tabuada, P. (2012). An introduction to event-triggered and self-triggered control. In *Proceedings of IEEE conference on decision and control* (pp. 3270–3285). IEEE.

International Society of Automation (2009). Wireless systems for industrial automation: Process control and related applications, ISA-100.11a-2009.

Isaksson, A. J., Harjunkoski, I., & Sand, G. (2017). The impact of digitalization on the future of control and operations. *Computers & Chemical Engineering*, *114*(7), 122–129. https://doi.org/10.1016/j.compchemeng.2017.10.037

Kiener, G. A., Lehmann, D., & Johansson, K. H. (2014). Actuator saturation and anti-windup compensation in event-triggered control. *Discrete Event Dynamic Systems*, *24*(2), 173–197. https://doi.org/10.1007/s10626-012-0151-1

Lehmann, D., & Johansson, K. H. (2012). Event-triggered PI control subject to actuator saturation. In *Proceedings of IFAC conference on advances in PID control* (pp. 430–435). Elsevier.

Lehmann, D., & Lunze, J. (2011). Extension and experimental evaluation of an event-based state-feedback approach. *Control Engineering Practice*, *19*(2), 101–112. https://doi.org/10.1016/j.conengprac.2010.10.003

Lindberg, C. F., & Isaksson, A. J. (2015). Comparison of different sampling schemes for wireless control subject to packet losses. In *Proceedings of International conference on event-based control, communication and signal processing* (pp. 1–8). IEEE.

Löfberg, J. (2004). YALMIP: A toolbox for modeling and optimization in MATLAB. In *Proceedings of IEEE international symposium on computer-aided control system design* (pp. 284–289). IEEE.

Moreira, L. G., Groff, L. B., Gomes da Silva Jr., J. M., & Tarbouriech, S. (2019). PI event-triggered control under saturating actuators. *International Journal of Control*, 92(7), 1634–1644. https://doi.org/10.1080/00 207179.2017.1404131

Norgren, T., Styrud, J., Isaksson, A. J., Åkerberg, J., & Lindh, T. (2012). Industrial evaluation of process control using non-periodic sampling. In *Proceedings of IEEE conference on emerging technologies and factory automation* (pp. 1–8). IEEE.

Park, P., Ergen, S. C., Fischione, C., Lu, C., & Johansson, K. H. (2018). Wireless network design for control systems: A survey. *IEEE Communications Surveys & Tutorials*, 20(2), 978–1013. https://doi.org/10.1109/COMST. 2017.2780114

Reimann, S., Van, D. H., Al-Areqi, S., & Liu, S. (2015). Stability analysis and PI control synthesis under event-triggered communication. In *Proceedings of European control conference* (pp. 2174–2179). IEEE.

Samad, T., McLaughlin, P., & Lu, J. (2007). System architecture for process automation: Review and trends. *Journal of Process Control*, 17(3), 191–201. https://doi.org/10.1016/j.jprocont.2006.10.010

Seborg, D. E., Mellichamp, D. A., Edgar, T. F., & Doyle III, F. J. (2010). *Process dynamics and control*. John Wiley & Sons.

Selivanov, A., & Fridman, E. (2016). Observer-based input-to-state stabilization of networked control systems with large uncertain delays. *Automatica*, 74(7), 63–70. https://doi.org/10.1016/j.automatica.2016. 07.031

Selivanov, A., & Fridman, E. (2018). Sampled-data implementation of derivative-dependent control using artificial delays. *IEEE Transactions on Automatic Control*, 63(10), 3594–3600. https://doi.org/10.1109/ TAC.9

Song, J., Mok, A. K., Chen, D., Nixon, M., Blevins, T., & Wojsznis, W. (2006). Improving PID control with unreliable communications. In *Proceedings of ISA EXPO technical conference* (pp. 17–19). ISA.

Tiberi, U., Araújo, J., & Johansson, K. H. (2012). On event-based PI control of first-order processes. In *Proceedings of IFAC conference on advances in PID control* (pp. 448–453). Elsevier.

Tiberi, U., Lindberg, C. F., & Isaksson, A. J. (2012). Dead-band self-triggered PI control for processes with dead-time. In *Proceedings of IFAC conference on advances in PID control* (pp. 442–447). Elsevier.

Wang, X., Yu, H., & Hao, F. (2017). Observer-based disturbance rejection for linear systems by aperiodical sampling control. *IET Control Theory & Applications*, 11(10), 1561–1570. https://doi.org/10.1049/cth2. v11.10

Appendices

Appendix 1. Proof of Lemma 3.1

Before presenting the proof, we introduce the following lemma.

Lemma A.1 (Selivanov and Fridman (2016)): *Let* $z : [a, b] \to \mathbb{R}^n$ *be an absolutely continuous function with a square integrable first order derivative such that* $z(a) = 0$ *or* $z(b) = 0$. *Then for any* $\alpha > 0$ *and* $W \in \mathbb{S}^n_{++}$, *the following inequality holds:*

$$\int_a^b e^{2\alpha t} z^\top(t) W z(t)\, dt \leq e^{2|\alpha|(b-a)} \frac{4(b-a)^2}{\pi^2} \int_a^b e^{2\alpha t} \dot{z}^\top(t) W \dot{z}(t)\, dt.$$

Now, we derive the stability condition of the system (12) with $\xi(t) \equiv 0$. Consider the functional

$$V = V_0 + V_{W_0} + \sum_{i \in \mathcal{N}} V_{W_i} + \sum_{i \in \mathcal{N}} V_{\bar{W}_i} + \sum_{i \in \mathcal{N}} V_{R_i} \tag{A1}$$

where

$$V_0 \triangleq x(t)^\top P x(t),$$

$$V_{W_0} \triangleq h_0^2 e^{2\alpha h_0} \int_{t_k}^t e^{-2\alpha(t-s)} \dot{x}(s)^\top W_0 \dot{x}(s)\, ds$$
$$\quad - \frac{\pi^2}{4} \int_{t_k}^t e^{-2\alpha(t-s)} \delta_0^\top(s) W_0 \delta_0(s)\, ds,$$

$$V_{W_i} \triangleq (h_0 + h_i)^2 e^{2\alpha(h_0+h_i)} \int_{s_i(t_k)}^t e^{-2\alpha(t-s)} \dot{x}(s)^\top W_i \dot{x}(s)\, ds$$
$$\quad - \frac{\pi^2}{4} \int_{s_i(t_k)}^t e^{-2\alpha(t-s)} \delta_i^\top(s) W_i \delta_i(s)\, ds,$$

$$V_{\bar{W}_i} \triangleq (h_0 + h_i)^2 e^{2\alpha(h_0+h_i)} \int_{s_i(t_k)-h_i}^t e^{-2\alpha(t-s)} \dot{x}(s)^\top \bar{W}_i \dot{x}(s)\, ds$$
$$\quad - \frac{\pi^2}{4} \int_{s_i(t_k)-h_i}^t e^{-2\alpha(t-s)} \bar{\delta}_i^\top(s) \bar{W}_i \bar{\delta}_i(s)\, ds,$$

$$V_{R_i} \triangleq \int_{t-h_i}^t e^{-2\alpha(t-s)} x^\top(s) R_i x(s)\, ds$$
$$\quad + h_i \int_{-h_i}^0 \int_{t+\theta}^t e^{-2\alpha(t-s)} \dot{x}^\top(s) R_i \dot{x}(s)\, ds\, d\theta,$$

with $\delta_0(t) \triangleq x(t_k) - x(t)$, $\delta_i(t) \triangleq x(s_i(t_k)) - x(t)$ and $\bar{\delta}_i(t) \triangleq x(s_i(t_k) - h_i) - x(t)$. Using Lemma A.1, we have

$$(t-t_k)^2 e^{2\alpha(t-t_k)} \int_{t_k}^t e^{-2\alpha(t-s)} \dot{x}^\top(s) W_0 \dot{x}(s)\, ds$$
$$- \frac{\pi^2}{4} \int_{t_k}^t e^{-2\alpha(t-s)} (x(s) - x(t_k))^\top(t) W_0 (x(s) - x(t_k))\, ds \geq 0.$$

Then $t - t_k \leq h_0$ gives

$$h_0^2 e^{2\alpha h_0} \int_{t_k}^t e^{-2\alpha(t-s)} \dot{x}^\top(s) W_0 \dot{x}(s)\, ds$$
$$- \frac{\pi^2}{4} \int_{t_k}^t e^{-2\alpha(t-s)} (x(s) - x(t_k))^\top(t) W_0 (x(s) - x(t_k))\, ds \geq 0,$$

which leads to $V_{W_0} \geq 0$. In the same way, we have $V_{W_i} \geq 0$ and $V_{\bar{W}_i} \geq 0$ as

$$t - s_i(t_k) = t - t_k + (t_k - s_i(t_k)) \leq h_0 + h_i.$$

We take the derivatives of each term

$$\dot{V}_0 + 2\alpha V_0 = x^\top(t)(P\bar{A} + \bar{A}^\top + 2\alpha P)x(t) + 2\sum_{i \in \mathcal{N}} x^\top(t) P A_i x(t-h_i)$$
$$\quad + 2\sum_{i=0}^N x^\top(t) P A_i \delta(t) + 2\sum_{i \in \mathcal{N}} x^\top(t) P \bar{A}_i \bar{\delta}(t),$$

$$\dot{V}_{W_0} + 2\alpha V_{W_0} = h_0^2 e^{2\alpha h_0} \dot{x}^\top(t) W_0 \dot{x}(t) - \frac{\pi^2}{4} \delta_0^\top(t) W_0 \delta_0(t),$$

$$\dot{V}_{W_i} + 2\alpha V_{W_i} = (h_0 + h_i)^2 e^{2\alpha(h_0+h_i)} \dot{x}^\top(t) W_i \dot{x}(t) - \frac{\pi^2}{4} \delta_i^\top(t) W_i \delta_i(t),$$

$$\dot{V}_{\bar{W}_i} + 2\alpha V_{\bar{W}_i} = (h_0 + h_i)^2 e^{2\alpha(h_0+h_i)} \dot{x}^\top(t) \bar{W}_i \dot{x}(t)$$
$$\quad - \frac{\pi^2}{4} e^{-2\alpha h_i} \bar{\delta}_i^\top(t) \bar{W}_i \bar{\delta}_i(t).$$

By Jensen's inequality (Fridman, 2014), we have

$$-\int_{t-h_i}^t \dot{x}^\top(s) R_0 \dot{x}(s)\, ds \leq \frac{1}{h_i} \int_{t-h_i}^t \dot{x}^\top(s)\, ds R_0 \int_{t-h_i}^t \dot{x}(s)\, ds.$$

Then

$$\dot{V}_{R_i} + 2\alpha V_{R_i} \leq x^\top(t)(Q_i - e^{-2\alpha h_i} R_i)x(t) + 2e^{-2\alpha h_i} x^\top(t) R_i x(t-h_i)$$
$$\quad - e^{-2\alpha h_i} x^\top(t-h_i)(Q_i + R_i)x(t-h_i) + h_i^2 \dot{x}^\top(t) R_i \dot{x}(t).$$

Taking

$$\phi(t)^\top(t) \triangleq [x^\top(t), x^\top(t-h_1), \ldots, x^\top(t-h_N), \delta_0^\top(t), \delta_1^\top(t), \ldots, \delta_N^\top(t),$$
$$\bar{\delta}_1^\top(t), \ldots, \bar{\delta}_N^\top(t)],$$

we have

$$\dot{V} + 2\alpha V = \phi^\top(t)\Phi'\phi(t) + \dot{x}^\top(t)S\dot{x}(t)$$

where

$$\Phi' \triangleq \begin{bmatrix} \Phi_{11} & \cdots & \cdots & \Phi_{1(3N+2)} \\ * & \ddots & & \vdots \\ \vdots & \ddots & \ddots & \vdots \\ * & \cdots & * & \Phi_{(3N+2)(3N+2)} \end{bmatrix}.$$

By Schur complements, we have that $\dot{V} + 2\alpha V < 0$ if $\Phi < 0$.

Appendix 2. Proof of Theorem 3.1

First, note that by the event-triggering condition (8), for some $w \geq 0$, we have

$$w\sigma u^\top(t)\Omega u(t) - w\xi^\top(t)\Omega\xi(t) \geq 0. \tag{A2}$$

Introducing the functional (A1) gives

$$\dot{V} + 2\alpha V \leq \dot{V} + 2\alpha V + w\sigma u^\top(t_k)\Omega u(t_k) - w\xi^\top(t)\Omega\xi(t).$$

Then

$$\dot{V} + 2\alpha V \leq \phi^\top(t)\Phi'\phi(t) + x^\top(t)PB\xi(t) + \xi^\top(t)B^\top Px(t)$$
$$+ \dot{x}^\top(t)S\dot{x}(t) + w\sigma u^\top(t_k)\Omega u(t_k) - w\xi^\top(t)\Omega\xi(t)$$

$$= \begin{bmatrix} \phi^\top(t) & \xi^\top(t) \end{bmatrix} \begin{bmatrix} & & & \vdots & PB \\ & \Phi' & & \vdots & 0 \\ & & & \vdots & \vdots \\ & & & \vdots & 0 \\ \hdashline * & * & \cdots & * & -w\Omega \end{bmatrix} \begin{bmatrix} \phi(t) \\ \xi(t) \end{bmatrix}$$

$$+ \dot{x}^\top(t)S\dot{x}(t) + w\sigma u^\top(t_k)\Omega u(t_k).$$

Substituting $u(t_k) = K_0 x(t_k) + K_i x(s_i(t_k)) + \bar{K}_i x(s_i(t_k) - h_i)$ into this, and applying Schur complements, we have $\dot{V} + 2\alpha V < 0$ if $\Psi < 0$.

Appendix 3. Proof of Theorem 3.3

We apply a coordinate transformation $\bar{\mathbf{x}}(t) = \mathbf{x}(t) - \mathbf{x}_e^*$. Then the system (21) can be rewritten as

$$\dot{\bar{\mathbf{x}}}(t) = \mathbf{A}\bar{\mathbf{x}}(t) + \mathbf{A}_0\bar{\mathbf{x}}(t_k) + \sum_{i\in\mathcal{N}} \mathbf{A}_i\bar{\mathbf{x}}(s_i(t_k)) + \sum_{i\in\mathcal{N}} \bar{\mathbf{A}}_i\bar{\mathbf{x}}(s_i(t_k) - h_i) + \mathbf{B}\xi(t). \tag{A3}$$

Consider the functional

$$\mathbf{V} = V_0 + V_{\mathbf{W_0}} + \sum_{i\in\mathcal{N}} V_{\mathbf{W_i}} + \sum_{i\in\mathcal{N}} V_{\tilde{\mathbf{W}}_i} + \sum_{i\in\mathcal{N}} V_{\mathbf{R_i}} \tag{A4}$$

where $V_0, V_{\mathbf{W_0}}, V_{\mathbf{W_i}}, V_{\tilde{\mathbf{W}}_i}$, and $V_{\mathbf{R_i}}$ are given by replacing P, W_0, W_i, Q_i, R_i in the functional (A1) by $\mathbf{P}, \mathbf{W}_0, \mathbf{W}_i, \mathbf{Q}_i, \mathbf{R}_i$. Then

$$\dot{\mathbf{V}} + 2\alpha\mathbf{V} \leq \dot{V} + 2\alpha V + w\sigma (u(t_k) - \mathbf{u}_c(t_k))^\top \Omega (u(t_k) - \mathbf{u}_c(t_k))$$
$$- w\xi^\top(t)\Omega\xi(t). \tag{A5}$$

Using

$$\mathbf{x}_e(t_k) - \mathbf{x}_e^* = \tilde{\mathbf{A}}^{-1}\mathbf{B}_D e_d(t_k)$$
$$= \tilde{\mathbf{A}}^{-1}\mathbf{B}_D\mathbf{E}\mathbf{x}(t_k)$$
$$= \tilde{\mathbf{A}}^{-1}\mathbf{B}_D\mathbf{E}\bar{\mathbf{x}}(t_k),$$

where the last equality holds since $\mathbf{E}\mathbf{x}_e^* = 0$, we have

$$u(t_k) - \mathbf{u}_c(t_k) = \mathbf{F}_0\bar{\mathbf{x}}(t_k) + \sum_{i\in\mathcal{N}} \left[\mathbf{K}_i\bar{\mathbf{x}}(s_i(t_k)) + \bar{\mathbf{K}}_i\bar{\mathbf{x}}(s_i(t_k) - h_i) \right].$$

Substituting this into (A5) and following the proof of Theorem 3.1 for the system (A3), we have that (21) is exponentially stable with decay rate α.